

Thermodynamic and Kinetic Behavior of B and Na Through the Contact of B-Doped Silicon with Na₂O-SiO₂ Slags

JAFAR SAFARIAN, GABRIELLA TRANELL, and MERETE TANGSTAD

Boron (B) is the most problematic impurity to be removed in the processes applied for the production of solar grade silicon. Boron removal from liquid silicon by sodium-silicate slags is experimentally studied and it is indicated that B can be rapidly removed within short reaction times. The B removal rate is higher at higher temperatures and higher Na₂O concentrations in the slag. Based on the experimental results and thermodynamic calculations, it is proposed that B removal from silicon phase takes place through its oxidation at the slag/Si interfacial area by Na₂O and that the oxidized B is further gasified from the slag through the formation of sodium metaborate (Na₂B₂O₄) at the slag/gas interfacial area. The overall rate of B removal is mainly controlled by these two chemical reactions. However, it is further proposed that the B removal rate from silicon depends on the mass transport of Na in the system. Sodium is transferred from slag to the molten silicon through the silicothermic reduction of Na₂O at the slag/Si interface and it simultaneously evaporates at the Si/gas interfacial area. This causes a Na concentration rise in silicon and its further decline after reaching a maximum. A major part of the Na loss from the slag is due to its carbothermic reduction and formation of Na gas.

DOI: 10.1007/s11663-013-9823-y

© The Author(s) 2013. This article is published with open access at Springerlink.com

I. BACKGROUND

ELEMENTAL silicon is produced through carbothermic reduction of quartz in the electric arc furnace, the product being metallurgical grade silicon (MG-Si), which is the basis of many metallurgical, chemical, and electrical applications. MG-Si contains about 99 wt pct Si with impurities such as Fe, Al, Ti, Ca, B, and P.^[1] Solar Grade Silicon (SoG-Si) with more than 6 N (+99.9999) purity is produced from MG-Si and it is the feedstock for the production of silicon solar cells. Ultrahigh pure silicon with around 11 N purity, which is called Electronic Grade Silicon (EG-Si), is used for the fabrication of electronic devices.^[1] A majority of SoG-Si and all the EG-Si existing in the market are currently produced from MG-Si through the *Siemens process* or the newly developed *fluid bed reactor (FBR) technology*. In these chemical processes, pure silicon is deposited on rods or seeds from a gas phase, which is produced from MG-Si and contains gaseous compounds of silicon such as SiHCl₃ or SiH₄. The Siemens process in particular is an expensive process with regard to high energy consumption.^[2,3] The production of SoG-Si through *metallurgical refining processes* is more energy efficient and

environmentally friendly than the chemical route which in turn may encourage a faster growth of the global PV market. This has been the motivation for the development of several refining processes such as the *ELKEM Solar Silicon (ESS) process* in Norway, the *NS Solar process* in Japan, *Chinese metallurgical routes* such as those of *Shanghai Propower* and *Ningxia*, and the *Photosil process* in France.^[3] In all these processes, MG-Si is refined through the combination of a few sub-processes to produce SoG-Si. Almost all the present impurities in MG-Si except B and P can be removed by directional solidification, which is usually a final key process step in the metallurgical approach. Boron is the most difficult element to remove by directional solidification due to its large distribution coefficient between solid and liquid phases, which is $K_B = 0.8$.^[4] In order to remove this impurity, many potential processes have been studied such as slag refining, plasma refining, gas refining, solvent refining, leaching, *etc.*^[3]

The application of slag refining processes for B removal from silicon has been extensively studied and commercialized in the ELKEM Solar Silicon process. Slag refining is well established in many metallurgical processes and therefore its application is beneficial from a technical production point of view. Moreover, slag refining can be performed on a large scale, which makes it more economic than many other process candidates, which are not as scalable. The potential of slags for B removal includes silicate slag compositions such as CaO-SiO₂,^[5-10] CaO-Ca F₂-SiO₂,^[6,8,11,12] CaO-BaO-SiO₂,^[6] CaO-MgO-SiO₂,^[5,6,13] CaO-Al₂O₃-SiO₂,^[14] CaO-Na₂O-SiO₂,^[14,15] Al₂O₃-CaO-MgO-SiO₂,^[16] Al₂O₃-BaO-SiO₂,^[16] and Al₂O₃-CaO-MgO-SiO₂.^[16] The thermodynamic equilibrium for B distribution between liquid silicon and molten slags has been most

JAFAR SAFARIAN, Researcher, is with the SINTEF Materials and Chemistry, Trondheim, Norway. Contact e-mail: Jafar.Safarian@sintef.no GABRIELLA TRANELL, Associate Professor, and MERETE TANGSTAD, Professor, are with the Department of Materials Science and Engineering, Norwegian University of Science and Technology (NTNU), Trondheim, Norway.

Manuscript submitted November 14, 2012.

Article published online March 7, 2013.

studied and the ratio of the concentrations of B in slag and silicon phases, the distribution coefficient denoted L_B ($L_B = \frac{(\text{pct B})}{[\text{wt pct B}]}$), has been determined. The thermodynamic parameter L_B is mainly dependant on temperature and slag chemical composition. In general, L_B is increased with increasing temperature as been observed through the studies using CaO-SiO₂ slags,^[6] CaO-CaF₂-SiO₂ slags,^[6,12] and CaO-Na₂O-SiO₂ slags.^[14,15] The relationship between L_B and slag chemical composition is complicated and L_B values in a wide range from 0.3 for CaO-SiO₂ slags^[6] to 9.3 using CaO-Al₂O₃-SiO₂ slags^[14] have been reported. Inspecting the literature data, it is seen that the measured L_B values for a given slag system are not in agreement. For instance, the L_B values reported by Teixeira *et al.*^[8] using CaO-SiO₂ slags are in the range of 2 to 5.5; L_B is in the minimum at CaO/SiO₂ = 0.85 and it is increased with both decreases and increases of the slag basicity. However, a much narrower L_B range for the same slag system has been recently observed, in which L_B is not significantly affected by the slag chemical composition and it increases minimally from 2.2 to 2.5 with increasing the basicity from 0.6 to 1.3.^[9] It has to be noticed that the analysis of B in low concentrations in both Si and slag phases is a challenge and this issue may be a reason for observing different results in similar experiments in addition to other sources of errors.

The kinetic studies on B removal by slags are more limited than the thermodynamic works and mass transfer coefficients such as $k_B = 1.4 \times 10^{-6}$ m/s for using CaO-SiO₂ slags at 1823 K (1550 °C),^[17] and larger values for the same slags and temperatures in the range of $k_B = 1.7 \times 10^{-6}$ m/s to 3.5×10^{-6} m/s^[18] have been reported. A relatively larger rate constant as $k_B = 4.3 \times 10^{-6}$ m/s has also been reported using CaO-MgO-SiO₂ slags.^[18] The mass transfer rate may or may not be connected to the observed relatively high L_B values ($L_B = 2.5$ to 3.5) using the same slag system.^[13]

Silicon refining studies using sodium oxide containing slag show varying results. Tanahashi *et al.*^[15] have shown that the addition of low amounts of Na₂O to CaO-SiO₂ slags increases the L_B value. They observed, however, much lower L_B values ($L_B = 0.03$) when they used 11 pct Na₂O-89 pct SiO₂ slags compared to the ternary Na₂O-CaO-SiO₂ slag systems, while higher L_B values are expected regarding the Na₂O effect on the ternary slag system. The silicon treatment by Na₂CO₃-SiO₂ mixtures carried out by Hu *et al.*,^[19] however, has shown significant B removal efficiencies. The different observations in these two works can be attributed to the compositional differences of the applied slags according to the Na₂O-SiO₂ binary phase diagram shown in Figure 1^[20]. Hu *et al.*^[19] used 30 to 50 pct Na₂CO₃ in their mixtures which provide slags in a complete molten state at the temperature of 1823 K (1550 °C), whereas the slag phase compositions chosen by Tanahashi *et al.* are in the two-phase region consisting of a solid SiO₂ and a liquid Na₂O-SiO₂ phase. The chemical reactions between these relatively viscose slags and liquid silicon may be limited, which could be the reason for Tanahashi *et al.* not observing significant B removal in their experiments.

In the present study, the removal of B from silicon by Na₂O-SiO₂ slags is studied applying experimental and theoretic approaches. Compared to the frequently used CaO-SiO₂ slags,^[5-10] the Na₂O-SiO₂ slags show relatively low melting points, lower density, lower surface tension, and lower viscosities.^[20] The latter two properties may provide better interfacial contact between the silicon and slag when Na₂O-SiO₂ slags are being used. When a Na₂O-SiO₂ slag is contacted with molten silicon, the metallurgical system is more complicated in comparison with many of the slag systems studied.^[5-18] This is due to the high vapor pressure of Na and lower stability of Na₂O than SiO₂ at elevated temperatures and in reducing conditions. Mass transport of B and Na to the gas phase has not been considered in the literature, while the distribution of B between the slag and silicon has been evaluated to establish the L_B values.^[15,19] However, when sodium-silicate slags are used, a three-phase reactive system consisting of a gas phase and the two slag and metal condensed phases has to be considered. The thermochemistry, kinetics, and mechanisms involved in the mass transport of Na and B among the silicon, slag, and gas phases are studied to gain an overall perspective on silicon refining through sodium-silicate slag treatment. In the experimental description of the present paper, the preparation of the Na₂O-SiO₂ slags and B-doped silicon and the applied method for interaction between them are briefly described. The measured chemical compositions for these reacted materials and the experimental observations are further presented. In order to discuss the obtained results and explain the changes in the concentrations of the silicon and slag phases, the thermochemistry of the reactions in the system is studied. Moreover, in order to evaluate the proposed reaction mechanisms, the literature data and fundamental thermodynamic and kinetic equations are employed.

II. EXPERIMENTAL PROCEDURE

Ultrahigh purity Electronic Grade Silicon (EG-Si) produced through the Siemens process with above 9 N purity was doped with pure boron (+99.98 pct), and silicon containing around 150 ± 3 ppmw boron was produced as determined by Inductively Coupled Plasma-Mass Spectroscopy (ICP-MS). This master Si-B alloy was prepared through the smelting of both elements in a high purity graphite crucible under inert gas flow (+99.999 pct Ar) in an induction furnace at 1773 K (1500 °C). The molten silicon was cast in a water-cooled copper mold for rapid solidification and to minimize the segregation of B. The solidified silicon was crushed down to +4.75 mm; the particles were then washed by HF to remove any surface impurities. Synthetic slags of Na₂O-SiO₂ mixtures were prepared with a similar method using Na₂CO₃ and SiO₂ mixtures to obtain the illustrated slags A, B, and C as seen in Figure 1. However, the smelting was done after slow heating for complete dissociation of sodium carbonate to Na₂O. The cast slag was crushed down to a fine powder in a tungsten carbide ring mill to obtain a homogeneous slag powder. The B concentration

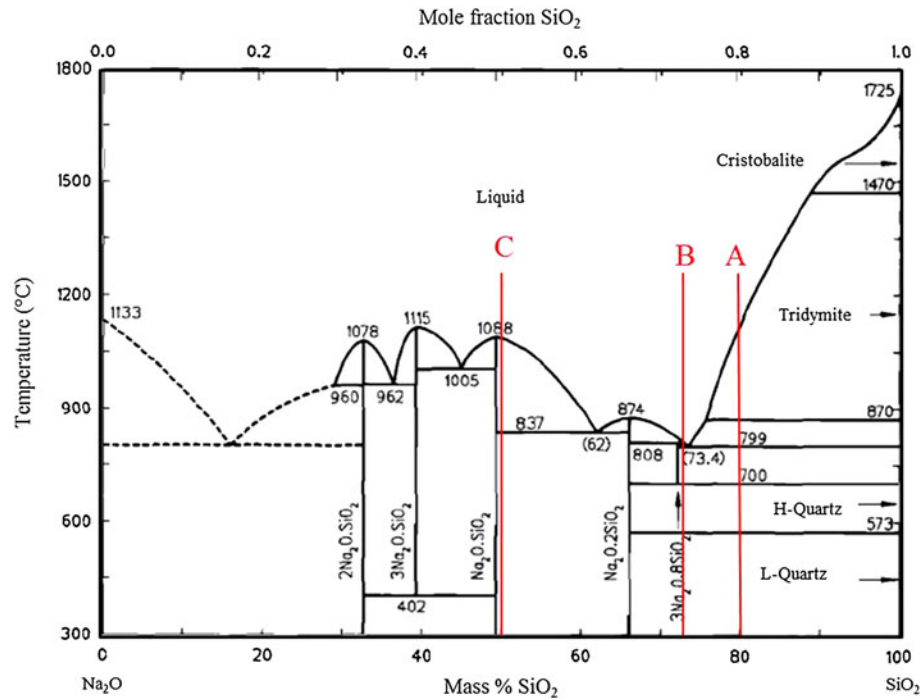


Fig. 1—Binary phase diagram of Na₂O-SiO₂ system and the selected slag compositions in the present study.

in the produced slag was low and around 0.64 ± 0.2 ppmw as determined by ICP-MS. A measured typical elemental composition of slag A (20 pct Na₂O-80 pct SiO₂) is 14.75 pct Na, 37.34 pct Si, 0.631 ppmw B, 622 ppmw Ca, 18.4 ppmw Mg, 247 ppmw Al, 1.4 ppmw Ba, and 3 ppmw P. The small amounts of the impurities are from the slag materials and the graphite crucible.

The slag refining experiments were carried out in a resistance furnace with a vertical graphite tube element. High purity graphite crucibles with 50 mm height, 40 mm outer diameter, and 32 mm inner diameter were used to cause a reaction of 15 g of silicon with 30 g slag. The silicon particles were first charged in the crucible and then the slag on top. The graphite crucible was located in the furnace on a graphite support and temperature at the crucible bottom was measured by thermocouple type B. The samples were heated at a rate of 25 K/minutes under Ar flow to the experimental temperatures of $1773 \text{ K} \pm 5 \text{ K}$ ($1500 \text{ }^\circ\text{C} \pm 5 \text{ }^\circ\text{C}$) and $1823 \text{ K} \pm 5 \text{ K}$ ($1550 \text{ }^\circ\text{C} \pm 5 \text{ }^\circ\text{C}$) followed by a constant temperature for the holding time specified. The experimental details are listed in Table I. The crucible was finally cooled down at a rate in the range of 105 C/minutes to 120 °C/minutes as monitored. The reacted silicon and slag phases were carefully separated through cutting the crucibles. They were further crushed and three samples of each phase were analyzed by ICP-MS to determine the concentrations in silicon and slag phases.

III. RESULTS

The experimental results and observations in this study are described as follows.

A. Chemical Analyses

The measured B and Na concentrations in the silicon samples post reaction are shown in Figure 2 vs the reaction times. As seen, the B concentration in silicon is decreased with refining time and it is affected by both the slag composition and the temperature. The B removal from silicon is faster at 1823 K (1550 °C) compared to 1773 K (1500 °C) when the same slag compositions are utilized. Figure 2 also shows that the B removal is faster for higher initial Na₂O concentrations. For instance, when the slag A at 1823 K (1550 °C) is used, around 52 pct of B is removed from the silicon in 15 minutes. However, when the slag C is used, around 91 pct of B is removed from the silicon within the same reaction time. The B concentration in the slag at 1773 K (1500 °C) is continuously increased within the applied refining times. However, for the experiments at 1823 K (1550 °C), the B concentration in the slag phase is increased initially to a maximum and then it is decreased. This may indicate the loss of B from the system and faster B loss at a higher temperature.

Compared to B concentration changes, a different behavior for Na is observed. The concentration of Na in silicon is initially increased to a maximum, followed by a continuous decrease. The concentration of Na in the slag phase is continuously decreased from the initial concentration (14.84 wt pct) in the experiments 1 to 6. An interesting point is the initial rapid Na loss from the slags, so that close Na contents in the slags are observed within almost the same reaction times. The presented data in Figure 2 indicate that although a large amount of Na is lost from the slag in a short time, only a small part is transferred to the Si melt.

Table I. Experimental Details in the Present Study

Experiment	Slag Compositions (wt pct)	Temperature (°C)	Refining Duration (min)
1	Slag A: 20 Na ₂ O-80SiO ₂	1773 (1500)	15
2	Slag A: 20 Na ₂ O-80SiO ₂	1773 (1500)	30
3	Slag A: 20 Na ₂ O-80SiO ₂	1773 (1500)	45
4	Slag A: 20 Na ₂ O-80SiO ₂	1773 (1500)	15
5	Slag A: 20 Na ₂ O-80SiO ₂	1773 (1500)	30
6	Slag A: 20 Na ₂ O-80SiO ₂	1773 (1500)	45
7	Slag B: 27.5 Na ₂ O-72.5SiO ₂	1773 (1500)	45
8	Slag C: 50 Na ₂ O-50SiO ₂	1773 (1500)	15

B. Other Observations

The main observations, which are important to gain a proper understanding about the mechanisms of the reactions, are summarized as follows.

1. Melt geometry

In all experiments, it was always observed that the solidified silicon has almost a ball shape form surrounded by the slag phase. A part of the silicon phase on top, *e.g.*, a cut spherical cap, is adjacent to the gas phase. This is seen in Figures 3(a) through (c), and the drawn schematic in Figure 3(d) represents the melt geometry.

2. Condensates on the element

A condensate of evaporated species was always observed in the furnace and over the top of the graphite element. This light green condensate caused the breakdown of the element after a few experiments. This may show a significant effect of the evaporated alkali species, Na compounds, on the graphite element. This confirms the significant Na loss from the system as mentioned above.

IV. DISCUSSION

Since the geometry of the system and the contact areas between the reactive phases are important, used later in kinetic calculations, a part is dedicated to study the smelting and the geometry of the system. The most possible involved mechanisms for the mass transport of Na and B species in the system are also studied in detail applying thermodynamic and kinetics principles.

A. Smelting and Interfacial Contacts

Three condense materials are in contact at elevated temperatures: Na₂O-SiO₂ slag, silicon, and solid carbon (graphite crucible). Based on the Na₂O-SiO₂ binary system illustrated in Figure 1, the applied slags start to melt from about 1073 K (800 °C) and they are completely molten at temperatures above 1423 K (1150 °C). This means that the slag phase is completely melted prior to silicon melting. Therefore, the slag flows down to the bottom of the crucible and over the silicon particles. This is enhanced due to the good wetting of both solid silicon and solid carbon by the molten

Na₂O-SiO₂ slags. Figures 3(a) through (c), which are after slag solidification in contact with solid silicon and the crucible wall, indicate the good wetting of these materials by the Na₂O-SiO₂ slags. A wetting angle of around $\theta = 20$ is estimated between slag A and graphite (Figure 3). On the other hand, a wetting angle of around $\beta = 54$ between slag A and solid silicon is estimated. During the slag melting, the high wettability of the graphite by the slag causes the spread of molten slag over the crucible wall. Further heating to the silicon melting point 1687 K (1414 °C) and above creates silicon droplets and these droplets are rapidly merging. This is confirmed through observing the single large ball shape silicon, even in the shortest experiments in 15 minutes. A very important point here is that there is no significant direct contact between the crucible wall and the molten silicon phase, whereas according to the literature there is good wetting between the graphite materials and molten silicon, and small wetting angles, *e.g.*, 5 to 30 deg have been observed.^[21] The reason may be the spread of the slag over the crucible wall prior to silicon melting so that it prevents significant contact between the molten silicon and the graphite crucible. According to Sato *et al.*,^[22] silicon density is approximately 2.56 g/cm³, 2.55 g/cm³, and 2.53 g/cm³ at 1687 K, 1773 K, and 1823 K (1414 °C, 1500 °C, and 1550 °C), respectively. According to the density measurements on Na₂O-SiO₂ slags,^[23] the density of slag is in the range of 2.16 g/cm³ to 2.28 g/cm³ for slags containing 30 to 70 pct SiO₂ and temperatures between 1373 K to 1773 K (1100 °C to 1500 °C). The slag should thus be expected to be on top of the metal. This is not the case, and the deviation from theory is believed to be due to the good wetting between the slag and graphite.

B. The Mass Transfer of Na

The Na₂O concentration changes in slag (Figure 2) show that the oxide is reduced from the slag. Moreover, a part of the produced Na is transferred to silicon, while a part is transferred to the gas phase. The possible reactions and mechanisms related to the observed Na concentration changes are studied as follows.

1. Na₂O reduction and Na transfer to silicon

Regarding the contact of the slag with both carbon and silicon, the Na₂O reduction takes place potentially through carbothermic and/or silicothermic reactions.

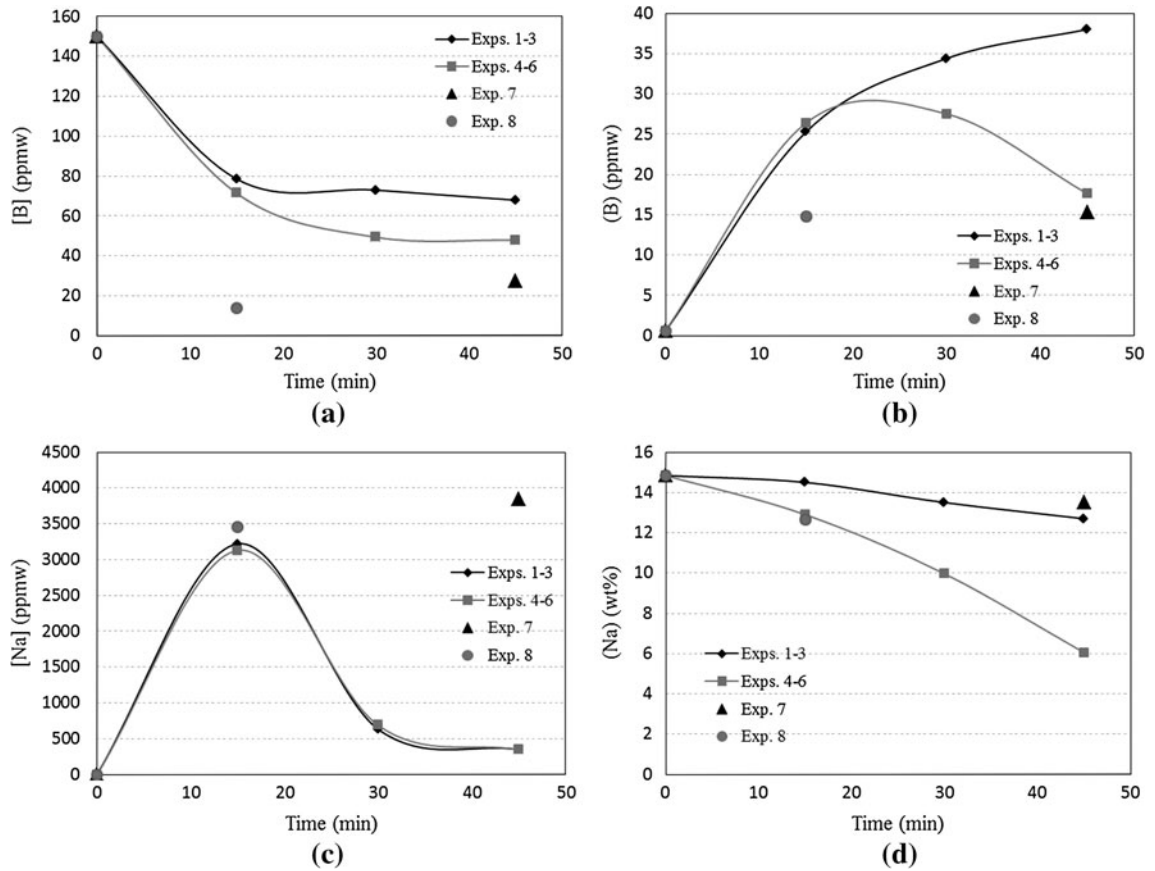
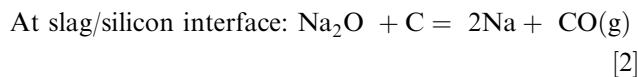
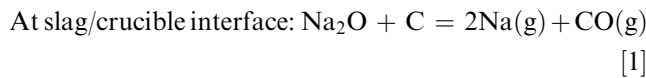


Fig. 2—Measured compositions of the silicon and slag phases after refining experiments.

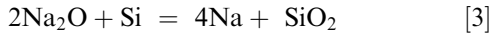
a. Carbothermic reduction of Na_2O . The carbothermic reduction of Na_2O occurs by both the crucible wall and the dissolved carbon in the molten silicon through the following reactions:



Since there is limited direct contact between the molten silicon and the crucible, the produced Na through Reaction [1] cannot be dissolved into the molten silicon. With regard to the much higher applied experimental temperatures than the Na boiling point 1156 K (883 °C), the produced Na at the slag/carbon interface has to be in the gaseous form. In contrast, the reduced Na_2O at the slag/silicon interface by the dissolved carbon in silicon can be transferred to the liquid silicon due to the low activity coefficient of Na in Si. The developed solar grade silicon database at NTNU/SINTEF^[24] gives Henrian activity coefficients of Na as 0.014 and 0.016 at 1773 K and 1823 K (1500 °C and 1550 °C), respectively. This significant negative deviation from the ideal solution causes, potentially, a relative high level of Na transport into the Si. We must

emphasize here that at this interface, a part of the reduced Na is evaporated due to the high vapor pressure of Na. The reduction of Na_2O by Reaction [2] is much less and negligible compared to Reaction [1] due to the small carbon solubility in silicon, which is based on the literature data^[25] of approximately 110 ppmw and 150 ppmw at 1773 K and 1823 K (1500 °C and 1550 °C), respectively. Moreover, the transfer of carbon into the silicon melt is limited due to the lack of direct contact between the liquid silicon and the crucible wall. Therefore, the main route for C transfer to the silicon melt can be *via* CO in the gas phase, which is produced through carbothermic Reaction [1], and can be dissociated at the silicon/gas interface. However, the rate of such a reaction is limited due to the use of Ar gas and also significant gas evolutions at the melt surface which make barriers for rapid CO mass transport to the silicon/gas interface. In short, we conclude here that Reaction [1] is the likely dominant carbothermic reduction reaction for Na_2O . In addition, Reactions [1] and [2] cannot cause significant Na transfer to the silicon (Figure 2) and another mechanism is involved as described below.

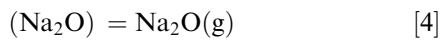
b. Silicothermic reduction of Na_2O . In addition to the carbothermic reduction, the silicothermic reduction of Na_2O from the slag takes place simultaneously at the silicon/slag interfacial area:



The standard Gibbs energy of oxidation of Si and Na at elevated temperatures was calculated by HSC Chemistry software version 7 and the results are shown in Figure 4. Since SiO_2 is more stable than Na_2O and Na has small activity in liquid silicon, Reaction [3] proceeds through the contact of Si and the slag. This liquid–liquid reaction takes place rapidly due to the contribution of only two liquids with direct contact. Considering negligible Na transfer into the silicon through the carbothermic reduction reactions as explained above, Reaction [3] is the likely dominant mechanism of Na transfer to the liquid silicon.

2. Na_2O loss through evaporation

In addition to the Na_2O depletion from the slag through reduction reactions, Na_2O evaporation from the slag has to be taken into account:



The slag phase contains Na_2O , SiO_2 , and a very low amount of B_2O_3 . The relationship between the standard vapor pressures of these oxides and temperature is shown in Figure 5. The presented dashed curve for

Na_2O is based on extrapolation of the measured Na_2O vapor pressures by Brewer and Mastick^[26] below 1190 K (917 °C). The measured vapor pressure data for B_2O_3 by Greene and Margrave^[27] are consistent with the calculated values by Elliot and Glierser.^[28] They are, however, relatively lower than the reported vapor pressures for B_2O_3 by Cole and Taylor.^[29] The two so far measured vapor pressures for SiO_2 by Porter and Chupka^[30] are lower than the calculated values here using the Antoine Equation for SiO_2 :

$$\log p_{(\text{mmHg})}^\circ = A - \frac{B}{T + C} \quad [5]$$

where A , B , and C are called Antoine coefficients and they are 9.87451, 16418.2, and 117.524,^[31] respectively, and T is temperature in degrees Celsius. The presented data in Figure 5 indicate that at elevated temperatures, above 1693 K (1420 °C), the evaporation potential of pure Na_2O is higher than pure SiO_2 . However, the evaporation potential of these compounds from the Na_2O - SiO_2 slags can be different depending on their activities. This issue is studied through the thermodynamic approach described below.

The above calculated vapor pressure data for Na_2O and SiO_2 are used to calculate their corresponding equilibrium partial pressures ($p_{\text{Na}_2\text{O}}^e$ and $p_{\text{SiO}_2}^e$) above the slag. This requires activity data of the Na_2O - SiO_2 slag

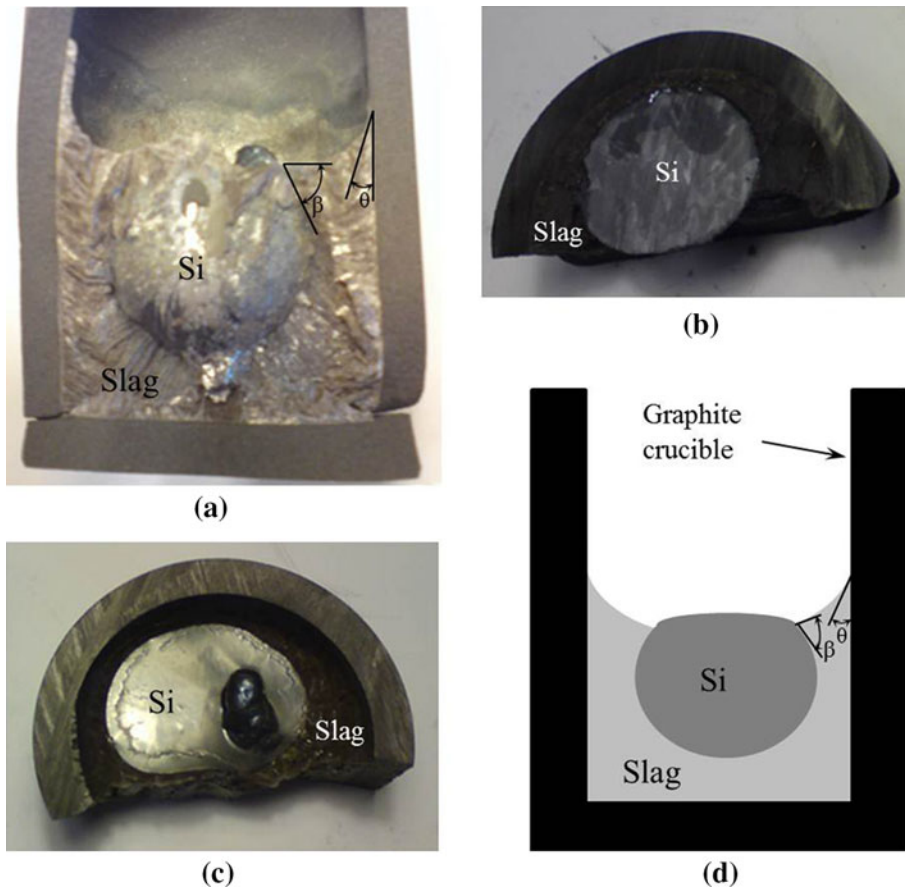


Fig. 3—A broken crucible after the experiment (a), the horizontal cross-sectional view from the middle of the crucible (b), a top view of the crucible (c), a schematic of the phases distribution (d).

system. The thermodynamic activities in Na₂O-SiO₂ slags were calculated with reference to the pure liquid states of the components employing FactSage thermodynamic software version 6.3 for 1773 K and 1823 K (1500 °C and 1550 °C) and the results are shown in Figure 6. In order to verify the calculated activities, selected experimentally measured activities in the literature^[32] are also shown in Figure 6. The measured Na₂O activities by Zaitsev *et al.* for the temperatures between 1373 K and 1673 K (1100 °C and 1400 °C) are consistent with regard to the dependence of $a_{\text{Na}_2\text{O}}$ on temperature as observed by Zaitsev *et al.*^[32] and recently Abdelouhab *et al.*^[33]. This is confirmed considering the experimentally measured activities by Goto *et al.*^[34] for 1773 K (1500 °C), as seen in Figure 6. Considering the calculated activities and the calculated vapor pressures (dashed and dashed-point curves of Figure 5), $p_{\text{Na}_2\text{O}}^e$ and $p_{\text{SiO}_2}^e$ can be calculated as typically shown in Figure 7 for 1773 K (1500 °C) for a wide range of slag compositions. It is observed that $p_{\text{Na}_2\text{O}}^e$ is lower than $p_{\text{SiO}_2}^e$ for the slags containing less than about 55 pct Na₂O. This gives a very important message that Na₂O has lower evaporation potential than SiO₂ from the applied slag compositions in this study.

a. Kinetics of Na₂O evaporation from slag. The rate of Na₂O evaporation from the slag can be theoretically calculated by employing the Hertz–Knudsen Equation^[35]:

$$\dot{n}_{\text{Na}_2\text{O}}^{\text{max}} = \frac{\alpha(p_{\text{Na}_2\text{O}}^e - p_{\text{Na}_2\text{O}}^g)}{\sqrt{2\pi M_{\text{Na}_2\text{O}} RT}} \quad [6]$$

where $M_{\text{Na}_2\text{O}}$ is the molecular weight of Na₂O, R is the universal gas constant, and $p_{\text{Na}_2\text{O}}^g$ is the partial pressure of Na₂O in the gas phase. The evaporation coefficient α is a constant and it is usually smaller than unity. According to Shirai *et al.*,^[36] this coefficient can be in the range of 0.05 to 0.125 for Na₂O evaporation from the Na₂O-SiO₂ melts at 1573 K and 1673 K (1300 °C and

1400 °C). Assuming this coefficient as unity here (the possible largest value) and assuming negligible Na₂O pressure ($p_{\text{Na}_2\text{O}}^g$) in the gas, the maximum possible Na₂O evaporation rate can be calculated by Eq. [6]. Figure 8 shows the calculated results (curves) for a wide range of slag chemical compositions at the experimental temperatures. These maximum theoretic values are much smaller than the determined Na₂O loss rate from the experimental measurements shown by symbols in Figure 8, which are obtained by mass balance calculations. From a kinetic point of view, this significant difference may indicate that the Na₂O loss from the slag is not due to the Na₂O evaporation reaction. Both the thermodynamic and kinetic discussions here indicate that the rapid Na₂O loss is mainly attributed to the reduction reactions. Since much less Na is transferred to the melt compared to the total Na loss, the main mechanism for Na₂O depletion is the carbothermic Reaction [1] at the slag/graphite interface. It is worth noting that the mass balance calculations mentioned above were carried out assuming negligible silicon loss from the system (SiO₂ reduction to SiO gas). This is a fair approximation with regard to weighting of the crucibles before and after experiments and observing mass decreases close to the total Na₂O loss.

3. Na evaporation and Na mass transport path

As mentioned above, the produced Na through the silicothermic reduction Reaction [3] is partly evaporated at the silicon/slag interfacial area, and a part of the produced Na is dissolved into the silicon. However, the evaporation of the dissolved Na in Si is simultaneously occurring at the silicon/gas interface:



This Na evaporation is due to the much higher vapor pressure of Na compared to the silicon solvent, so that even the equilibrium vapor pressures of the dilute solutions of Na in silicon are significantly higher than

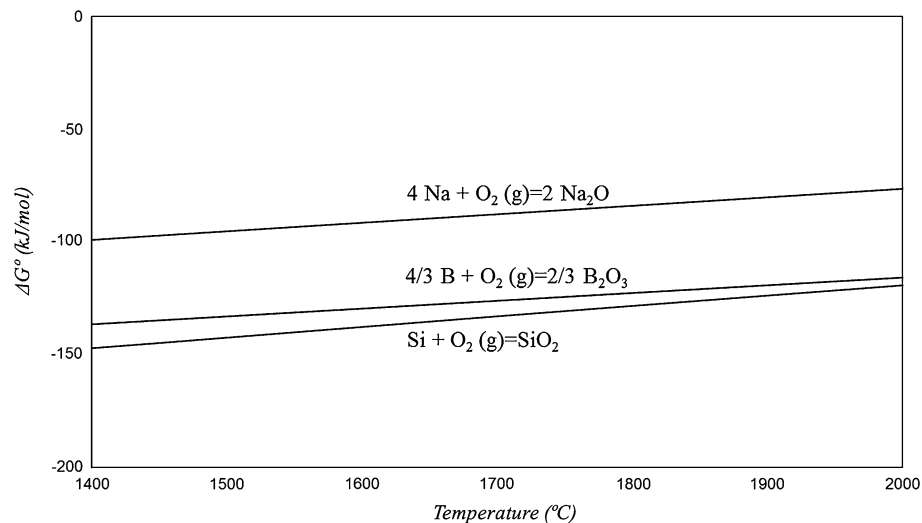


Fig. 4—The changes of the standard Gibbs free energy of oxidation of Na, B, and Si with temperature.

the silicon vapor pressure.^[35] The observed concentration changes of Na in Si (Figure 2) are attributed to the kinetics of Reactions [3] and [7]. When silicon is contacted with the slag, Reaction [3] is started and Na is transferred to the silicon melt, which causes the increase of Na concentration, while Na evaporation at the Si/gas interface is also taking place. With decreasing the Na₂O concentration in the slag, the rate of Reaction [3] is decreased due to the reaction driving force decline. Therefore, when this rate is equal to Na evaporation *via* Reaction [7], the Na concentration in silicon reaches its maximum. The Na concentration is decreased with longer refining times due to the higher rates of Reaction [7] compared to Reaction [3] as observed in Figure 2. Another mechanism which can explain the Na concentration drop after reaching the concentration hump can be the return of Na from the silicon phase to the slag due to the activity drop of Na₂O in the slag. In order to distinguish which of these two mechanisms causes the dissolved Na concentration drop, the thermodynamic equilibrium between the Si-Na melts and Na₂O-SiO₂ slags is considered. Given Reaction [3] at equilibrium, we may write

$$\frac{a_{\text{Na}}^4}{a_{\text{Si}}} = \frac{a_{\text{Na}_2\text{O}}^2}{a_{\text{SiO}_2}} \exp\left(\frac{-\Delta G_3^\circ}{RT}\right) \quad [8]$$

where a_i refers to the activity of component i . Assuming the ideal behavior for Si-Na solutions, the following relationships between the equilibrium concentration of Na in the melt (X_{Na}^e) and the slag thermodynamic properties is obtained:

$$\frac{X_{\text{Na}}^e}{1 - X_{\text{Na}}^e} = \left(\frac{a_{\text{Na}_2\text{O}}^2}{a_{\text{SiO}_2}} \exp\left(\frac{-\Delta G^\circ}{RT}\right) \right)^{\frac{1}{4}} \quad [9]$$

The solution results of this equation are shown in Figure 9 vs the changes of the slag chemical composition.

Obviously, the experimentally observed Na concentrations are much less than the approximate calculated equilibrium concentrations and the system is quite far from the equilibrium. It is worth mentioning that Si-Na melts show negative deviations from the ideal solution as mentioned before and the actual Na concentrations are even higher than those illustrated in Figure 9. Observing much lower Na concentrations in the melt than the equilibrium concentrations indicates that the return of the dissolved Na in liquid silicon to the slag is impossible. Therefore, we may conclude that the reduced Na by the silicothermic reduction is transferred to the Si/gas interface and then rapidly evaporated. The much lower Na concentration than the equilibrium concentration may also show the relatively fast mass transport of Na in Si and its fast evaporation at the silicon/gas interfacial area. Hence, the Na mass transport is mainly controlled by the kinetics of the reduction Reaction [3] at the silicon/slag interfacial area.

C. Boron Removal

The experimental results indicate that a large amount of B is removed from the silicon melt within short refining times. Therefore, sodium-silicate slags show high potential for deboronization of molten silicon. Boron has lower vapor pressure than silicon and it has been shown that the B removal from silicon through evaporation is not viable.^[35] Hence, the elimination of B from silicon takes place only at the silicon/slag interfacial area. Based on the obtained results and theoretic approaches, the B removal from silicon by the Na₂O-SiO₂ slags is studied as follows.

1. The rate of B removal from silicon

The dissolved B in silicon is oxidized by the slag and it is transferred to the slag in the form of B₂O₃.^[5-18] Considering a first-order reaction for the B oxidation at slag/silicon interface, we obtain

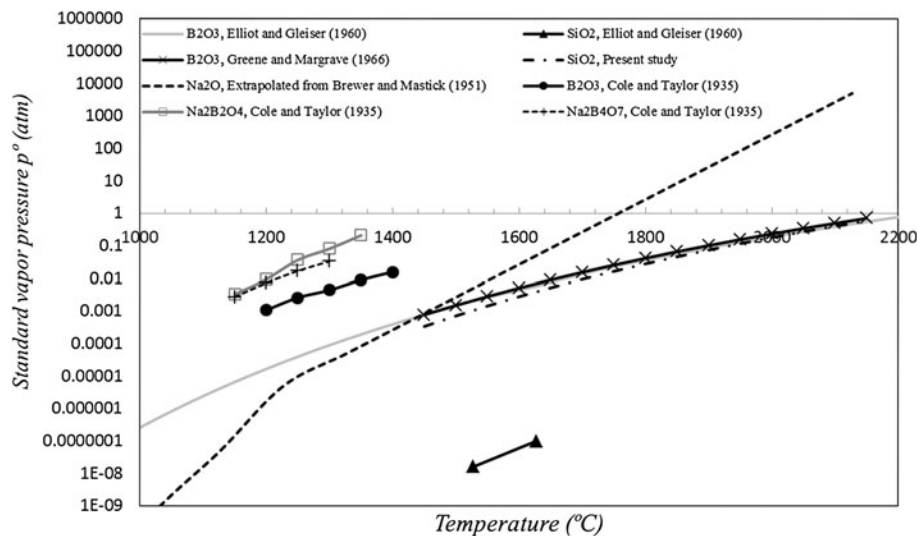


Fig. 5—The relationship between the saturated vapor pressures of Na₂O, SiO₂, and B compounds and temperature.

$$\ln \frac{C_B^i}{C_B} = \frac{A_{\text{Si/Slag}}}{V_{\text{Si}}} k_B t \quad [10]$$

where k_B is the rate constant, C_B^i and C_B are the B concentrations in silicon at initial and at refining time t , respectively. $A_{\text{Si/Slag}}$ is the Si/slag contact area and V_{Si} is the volume of the silicon melt. It is worth mentioning that the above equation has been derived assuming a negligible final B concentration in silicon, which is a fair approximation with the later discussions in this paper in which it will be shown that B can be almost completely removed by the applied experimental approach. Figure 10 shows the calculated rate constant values through the estimation of $A_{\text{Si/Slag}} \approx 13.7 \text{ cm}^2$ contact area with regard to the geometry of the system described above. It is observed that the rate constant for B removal by the slag A is in the range of 1.3×10^{-6} to 3.1×10^{-6} m/s for the experiments at 1773 K (1500 °C). The similar experiments at 1550 °C show little higher k_B values in the narrower range of 1.8×10^{-6} to 3.6×10^{-6} m/s. However, for the same reaction times, the k_B values are larger at 1823 K (1550 °C) than those at 1773 K (1500 °C). This indicates that the kinetics of B removal is increased with increasing temperature. For both experiential temperatures using slag A, the smaller k_B values are obtained for longer reaction times. This may be due to the changes in the slag chemical composition by time, and as such the B removal potential by $\text{Na}_2\text{O-SiO}_2$ slags is decreased with decreasing the Na_2O concentration in the slag. This is confirmed through the comparison of k_B values obtained for experiments 6 and 7 and those obtained for experiments 4 and 8. The comparison of k_B values with the concentration changes in Figure 2 shows that the rate of B removal is higher initially, when Na_2O content of the slag is high and Na mass transfer to silicon is fast. Thus, the B removal kinetics can be in direct relation to the Na_2O reduction from the slag *via* Reaction [3]. In order to clarify more details about the B removal,

the thermochemistry and mechanism of B oxidation by the slag are studied.

2. Chemistry and mechanism of B oxidation by the slag

As mentioned above, the B elimination from silicon takes place at the silicon/slag interfacial area. The possible reactions for B oxidation are

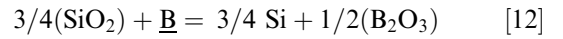
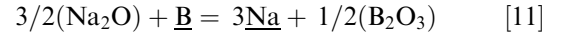


Figure 11 shows the calculated standard Gibbs free energy changes for the above reactions and it is observed that under standard conditions, in which pure substances are reacted and pure products are formed, Reaction [11] is favorable to occur rather than Reaction [12]. The B oxidation by SiO_2 is not expected, since SiO_2 is more stable than boron oxide (Figure 4). However, since the substances in Reactions [11] and [12] are not pure in our reactive system, the changes in the Gibbs free energies of the above reactions have to be studied by considering the activities in both silicon and slag phases:

$$\Delta G_{11} = \Delta G_{11}^\circ + RT \ln \frac{a_{\text{Na}}^3 a_{\text{B}_2\text{O}_3}^{1/2}}{a_{\text{B}} a_{\text{Na}_2\text{O}}^{3/2}} \quad [13]$$

$$\Delta G_{12} = \Delta G_{12}^\circ + RT \ln \frac{a_{\text{Si}}^{3/4} a_{\text{B}_2\text{O}_3}^{1/2}}{a_{\text{B}} a_{\text{SiO}_2}^{3/4}} \quad [14]$$

Rearranging the above equations, we obtain

$$\delta G_{11} = \Delta G_{11} - RT \ln \frac{a_{\text{B}_2\text{O}_3}^{1/2}}{a_{\text{B}}} = \Delta G_{11}^\circ + RT \ln \frac{a_{\text{Na}}^3}{a_{\text{Na}_2\text{O}}^{3/2}} \quad [15]$$

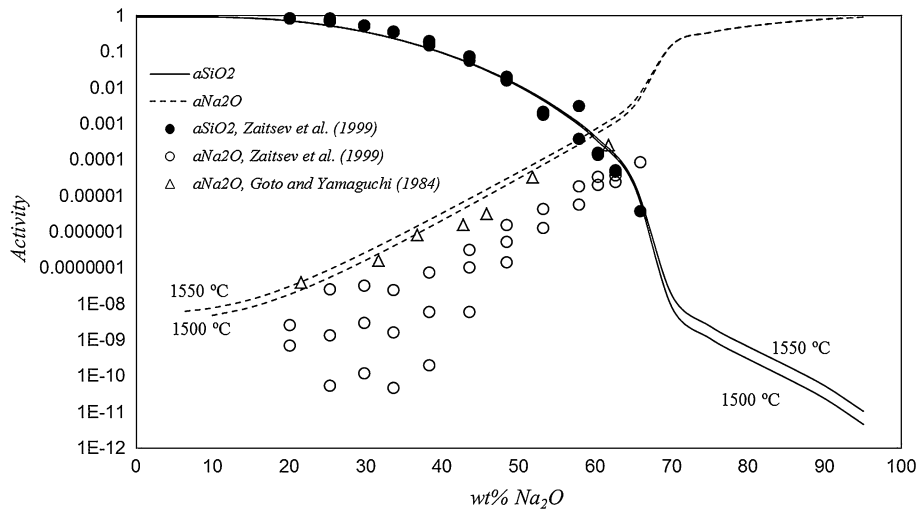


Fig. 6—Calculated activities and literature data for $\text{Na}_2\text{O-SiO}_2$ slags.

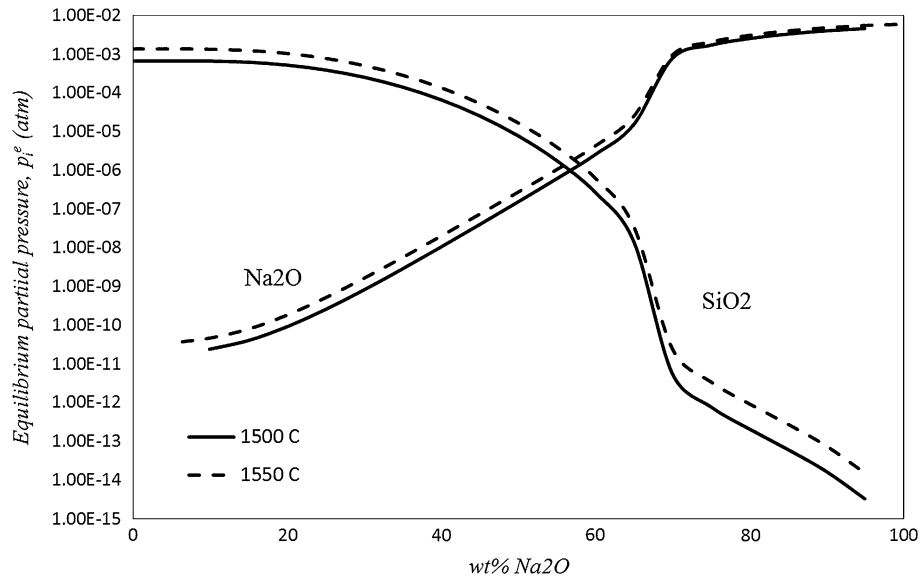


Fig. 7—Relationship between the equilibrium partial pressures of Na₂O and SiO₂ with the slag chemical composition.

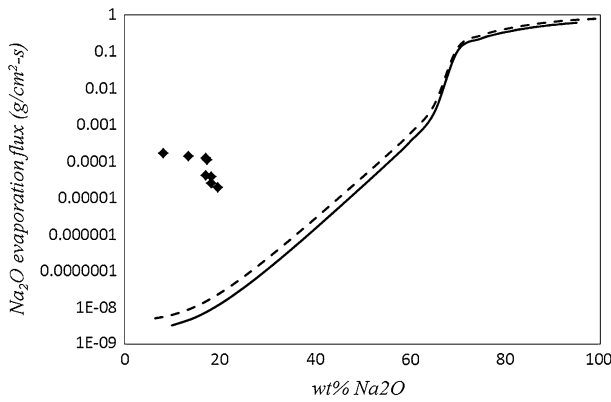


Fig. 8—Maximum possible evaporation flux of Na₂O from the slags (curves) and the determined fluxes for the experiments in the present study (symbols).

$$\delta G_{12} = \Delta G_{12} - RT \ln \frac{a_{B_2O_3}^{1/2}}{a_B} = \Delta G_{12}^\circ + RT \ln \frac{a_{Si}^{3/4}}{a_{SiO_2}^{3/2}} \quad [16]$$

Studying the changes of ΔG_{11} and ΔG_{12} instead of ΔG_{11} and ΔG_{12} is beneficial as the calculation of B and B₂O₃ activities in Si and slag phases is redundant since the same expression is subtracted from ΔG_{11} and ΔG_{12} . It is worth noting that it is difficult to calculate accurate $a_{B_2O_3}$ in very low concentrations in the slags. Based on the above calculated slag activities, the right hand side of the Eqs. [15] and [16] was calculated for dilute solutions of Na in Si ($a_{Si} \approx 1$) and the results are illustrated in Figure 12 for typical composition of $X_{Na} = 0.05$. The Henrian activity coefficient of Na in Si is $\gamma_{Na}^\circ = 0.014$ at 1773 K (1500 °C) as mentioned above. Obviously, the ΔG_{11} values are negative and significantly lower than the ΔG_{12} values for the same slag compositions. This means that the oxidation of the

dissolved B in Si takes place by Na₂O through Eq. [11], while it is impossible through Eq. [12].

When silicon is in contact with very low Na₂O-containing slags, the activity of Na₂O is subsequently low and therefore the B oxidation by SiO₂ must also be taken into account, depending on the B₂O₃ activities. Hence, there might be a critical concentration of Na (X_{Na}^{cr}) in Si and below that, B can be oxidized by SiO₂, while at higher concentrations, it is oxidized by Na₂O. This critical concentration can be determined by considering $\Delta G_{11} = \Delta G_{12}$ which gives

$$X_{Na}^{cr} = \frac{1}{\gamma_{Na}^\circ} \left\{ a_{Na_2O}^{3/2} \left[\frac{\Delta G_{12}^\circ - \Delta G_{11}^\circ}{RT} + \ln \left(\frac{a_{Si}^{3/4}}{a_{SiO_2}^{3/2}} \right) \right] \right\}^{1/3} \quad [17]$$

According to the above calculated activities for Na₂O-SiO₂ slags, a_{SiO_2} in rich silica slags is almost at unity, while Na₂O shows Henrian behavior. Regarding a_{Si} as unity, Eq. [17] can be simplified to

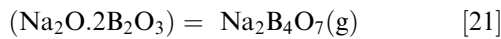
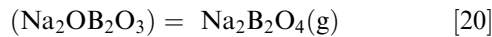
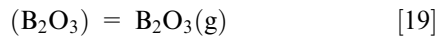
$$X_{Na}^{cr} = \frac{\gamma_{Na_2O}^\circ 1/2 (\Delta G_{12}^\circ - \Delta G_{11}^\circ)^{3/2}}{RT \gamma_{Na}^\circ} X_{Na_2O}^{1/2} \quad [18]$$

Considering $\gamma_{Na_2O}^\circ = 5 \times 10^{-8}$ at 1773 K (1500 °C) as calculated, the relationship between X_{Na}^{cr} and X_{Na_2O} is obtained as shown in Figure 13, where X_{Na}^{cr} is proportional to the square root of X_{Na_2O} . Since very small X_{Na}^{cr} values correspond to low Na₂O concentrations, we may conclude that the B oxidation from the Si melts, even to very low Na₂O concentrations in the slag, is taking place by Na₂O.

3. Boron loss from the slag

Based on the analysis results, there is a significant B loss into the gas phase, which is clearly seen for the experiments 4 to 6 (Figure 2). Mass balance calculations give us the B loss results shown in Figure 14. The extent of B loss in

experiments 1 to 3 at 1773 K (1500 °C) is decreased with longer reaction times and this is difficult to explain. However, the B loss is increased with increasing reaction time for the experiments at 1823 K (1550 °C) with a logical trend. Generally speaking, the extent of B loss is higher for the slags containing higher Na₂O contents and higher temperatures. For Exp. 8 with 50 pct Na₂O initially, more than 78 pct of B is lost from the condensed phases. Since B evaporation from liquid silicon is not possible,^[35] it may be concluded that the oxidized B at the Si/slag interfacial area diffuses into the slag phase and is further evaporated at the slag/gas interface. Although the evaporation of B₂O₃ from the system is possible, B₂O₃ may form complexes such as Na₂B₂O₄ and Na₂B₄O₇ with a significant amount of coexisting Na₂O^[19,29]. The possible evaporation reactions which cause the B loss are



According to Cole and Taylor,^[29] the vapor pressure of Na₂B₂O₄ is higher than B₂O₃ and Na₂B₄O₇ as seen in Figure 5. The boiling point of Na₂B₂O₄, 1707 K (1434 °C), is also lower than B₂O₃, 2133 K (1860 °C), and Na₂B₄O₇, 1848 K (1575 °C). Regarding higher B removal rates for higher Na₂O concentrations, it may be concluded that B removal is mainly occurring due to the evaporation of Na₂B₂O₄ at the slag/gas interfacial area. It is worth noting that Na₂B₄O₇ decomposes at high temperatures and the Na₂B₂O₄ gas is more stable.^[29]

D. Overall B Removal Mechanism and Rate-Limiting Steps

Considering the above discussions, the main reactions in the system can be presented schematically as

illustrated in Figure 15. Regarding the B mass transfer path in the system, the B removal is taking place through these process steps:

1. Mass transport of the dissolved B from the bulk silicon phase to the Si/slag interface; a melt boundary diffusion layer may exist adjacent to the interface;
2. The oxidation of B at the Si/slag interface by Na₂O;
3. The mass transfer of B₂O₃ to the slag/gas interfacial area; diffusion boundary layers may exist in the slag phase adjacent to the liquid silicon and gas phases;
4. Evaporation of Na₂B₂O₄ at slag/gas interface;
5. Mass transport of the Na₂B₂O₄ in the gas phase.

The dependence of the calculated k_B values on both slag composition and temperature (Figure 10) indicates that the process rate is dependent on the rate of process step (2). On the other hand, using higher Na₂O-containing slags indicates faster B elimination from the slag, which shows the contribution of process step (4) in the total kinetic behavior of B removals. This in turn provides larger driving force for the B oxidation in the system, step (2). Therefore, the refining process rate is dependent on the rate of the chemical reactions in both steps (2) and (4). The ratio of B

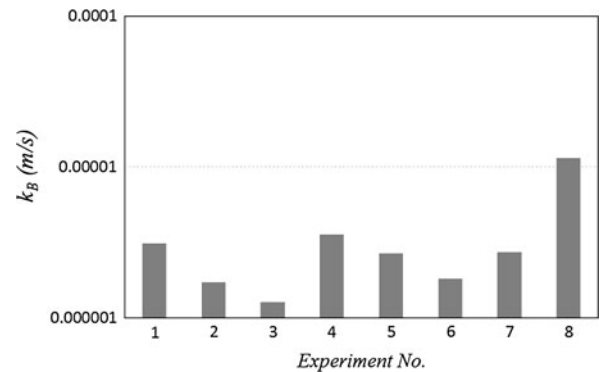


Fig. 10—Calculated rate constants for B removal from silicon melts.

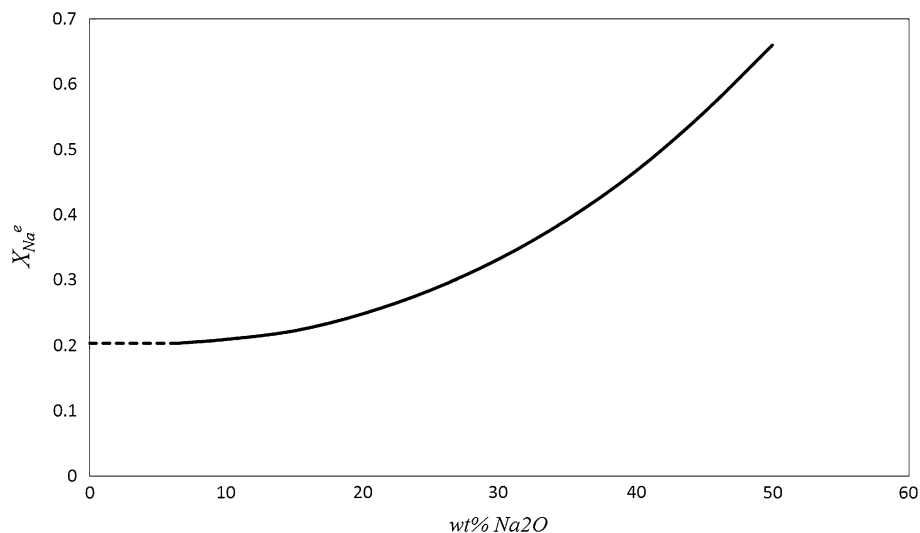


Fig. 9—Relationship between the equilibrium Na concentration in Si and slag chemical composition for the case of Si-Na ideal solutions.

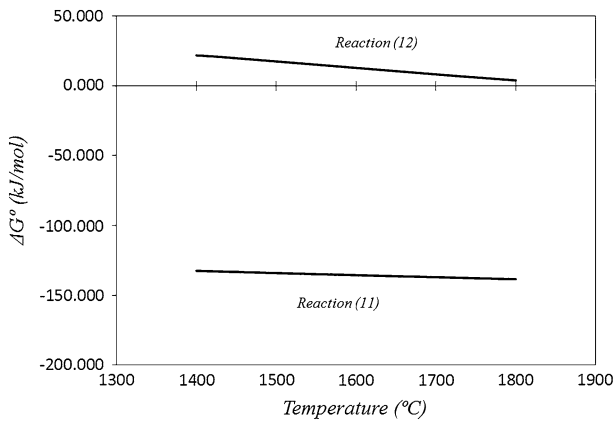


Fig. 11—The changes of the standard Gibbs free energy of Reactions [11] and [12] with temperature.

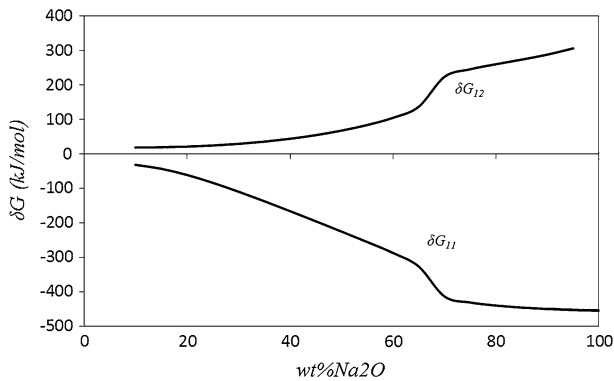


Fig. 12—The changes of ΔG_{11} and ΔG_{12} for Reactions [11] and [12] with the slag chemical composition for a given Na concentration in silicon ($X_{Na} = 0.05$).

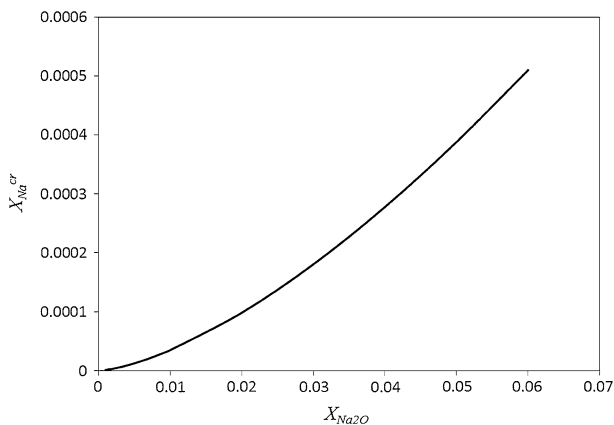


Fig. 13—Relationship between the X_{Na}^{cr} and slag chemical composition.

concentration in the slag over B concentration in Si ($wt\ pct\ B)/[wt\ pct\ B]$ for this reactive system was calculated for the experiments. We emphasize here that this parameter is not a thermodynamic parameter like L_B that was mentioned above. The illustrated results in Figure 16 show that when slag C is used, a significant

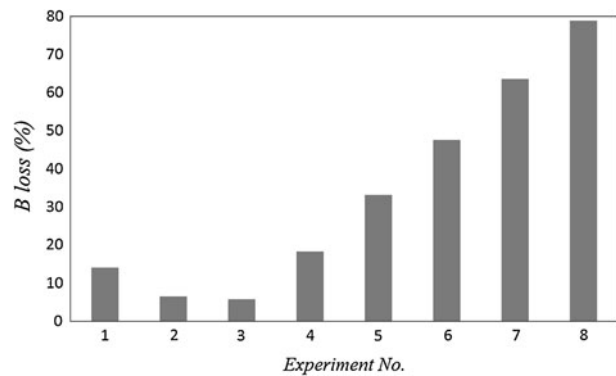


Fig. 14—The calculated B loss for the experiments 1 to 8.

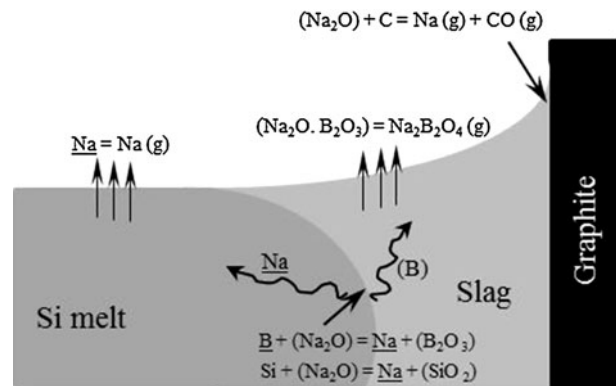


Fig. 15—Schematic of the mechanism of B removal, Na_2O reduction, and Na mass transport path in the silicon refining process by Na_2O-SiO_2 slags in graphite crucible.

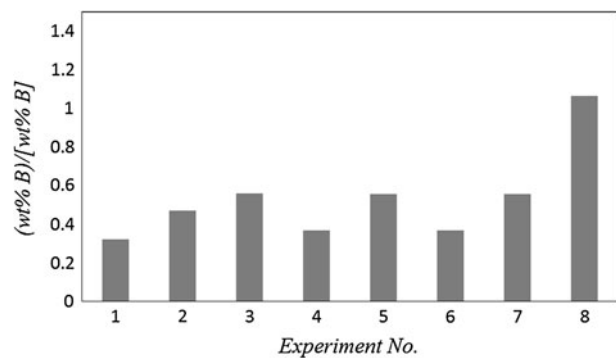


Fig. 16—Calculated $(wt\ pct\ B)/[wt\ pct\ B]$ values for experiments 1 to 8.

amount of B is rapidly transferred to the slag, while its transfer to the gas phase is slower so that a much higher $(wt\ pct\ B)/[wt\ pct\ B]$ ratio is obtained. This can indicate that the rate of process is less dependent on the process step (2) when high Na_2O concentrations are used, and step (4) becomes more important. In order to clarify more kinetics details and in particular the role of the other process steps, such as step (3), more precise experimental work is required.

V. CONCLUSIONS

The thermochemistry, kinetics, and mechanism of B removal from silicon by Na₂O-SiO₂ slags were studied through experimental work and an analytical approach. It was concluded that the dissolved B in silicon melt is oxidized by the Na₂O at the slag/silicon interfacial area. The transferred B to the slag is further removed at the slag/gas interface in the form of Na₂B₂O₄, which is a more volatile compound in comparison with B₂O₃ and Na₂B₄O₇. The overall B removal rate depends on the kinetics of these chemical reactions at the interfaces. The B removal rate increases with increasing the Na₂O concentration in the slag and also increasing temperature. Moreover, the kinetics of B removal is relative to the Na distribution and mass transport in the system. The Na content of the liquid silicon is rapidly increased through contact with the slag, and after reaching a maximum, it declines. The transferred Na in the silicon is evaporated at the Si/gas interface simultaneously with silicothermic Na₂O reduction at the slag/Si interface. However, Na₂O depletion from the slag is mainly related to the carbothermic reduction of Na₂O at the slag/graphite crucible contact area, while the Na₂O evaporation is negligible.

ACKNOWLEDGMENT

The authors acknowledge the funding provided through the BASIC project (191285/V30) by the Norwegian Research Council.

OPEN ACCESS

This article is distributed under the terms of the Creative Commons Attribution License which permits any use, distribution, and reproduction in any medium, provided the original author(s) and the source are credited.

REFERENCES

1. A. Schei, J. Kr. Tuset, and H. Tveit: *Production of High Silicon Alloys*, Trondheim, Tapir Forlag, 1998.
2. A.F.B. Braga, P.R. Zampieri, J.M. Bacchin, and P.R. Mei: *Sol. Energy Mater. Sol. Cells*, 2008, vol. 92, pp. 418–24.
3. J. Safarian, G. Tranell, and M. Tangstad: *Energy Procedia*, 2012, vol. 20, pp. 88–97.
4. R.H. Hopkins and A. Rohatgi: *J. Cryst. Growth*, 1986, vol. 75, pp. 67–79.
5. H.M. Liaw and F. Secco D'Aragona: *Solar Cells*, 1983, vol. 10, pp. 109–18.
6. K. Suzuki, T. Sugiyama, K. Takano, and N. Sano: *J. Jpn. Inst. Met.*, 1990, vol. 54, pp. 168–72.
7. T. Weiss and K. Schwerdtfeger: *Metall. Mater. Trans. B*, 1994, vol. 25B, pp. 497–504.
8. L.A.V. Teixeira, Y. Tokuda, T. Yokoi, and K. Morita: *ISIJ Int.*, 2009, vol. 49, pp. 777–82.
9. L.K. Jakobsson and M. Tangstad: *International Smelting Technology Symposium (Incorporating the 6th Advances in Sulfide Smelting Symposium)*, J.P. Downey, T.P. Battle, and J.F. White, eds., TMS, Orlando, FL, USA, 2012, pp. 179–14.
10. E. Krystad, J. Kline, M. Tangstad, and G. Tranell: *Ninth International Conference on Molten Slags, Fluxes and Salts (MOL-TEN12)*, Beijing, China, 2012.
11. J. Dietle: *Silicon Photovolt.*, 1987, vol. 2, pp. 285–352.
12. J. Cai, J.T. Li, W.H. Chen, C. Chen, and X.T. Luo: *Trans. Non-ferrous Met. Soc. China*, 2011, vol. 21, pp. 1402–06.
13. J. White, C. Allertz, K. Forwald, and D. Sichen: *Ninth International Conference on Molten Slags, Fluxes and Salts (MOL-TEN12)*, Beijing, China, 2012.
14. D.W. Luo, N. Liu, Y.P. Lu, G.L. Zhang, and T.J. Li: *Trans. Nonferrous Met. Soc. China*, 2011, vol. 21, pp. 1178–84.
15. M. Tanahashi, Y. Shinpo, T. Fujisawa, and C. Yamauchi: *J. Min. Mater. Proc. Inst. Jpn.*, 2002, vol. 118, pp. 497–505.
16. M.D. Johnston and M. Barati: *Sol. Energy Mater. Sol. Cells*, 2010, vol. 94, pp. 2085–90.
17. H. Nishimoto and K. Morita: *TMS*, 2011, vol. 1, pp. 701–08.
18. E. Krystad, S. Zhang, and G. Tranell: *EPD Congress 2012 (TMS)*, FI, USA, 2012, pp. 471–80.
19. Y. Hu, D. Lu, T. Lin, Y. Liu, B. Wang, C. Guo, Y. Sun, H. Chen, and Q. Li: *Adv. Mater. Res.*, 2011, vols. 156–157, pp. 882–85.
20. M. Allibert, R. Para, C. Saint-Jours, and M. Tmar: *Slag Atlas*, 2nd ed., Verlag Stahleisen GmbH, Dusseldorf, Germany, 1995.
21. A. Ciftja: *Solar silicon refining; Inclusions, smelting, filtration, wetting*, NTNU Trykk, Doctoral thesis, 2009, p. 103.
22. Y. Sato, T. Nishizuka, K. Hara, T. Yamamura, and Y. Waseda: *Int. J. Thermophys.*, 2000, vol. 21, p. 1463–71.
23. B.J. Keene and K.C. Mills: *Slag Atlas*, 2nd ed., Dusseldorf, Germany, Verlag Stahleisen GmbH, 1995, p. 325.
24. K. Tang, E.J. Øvrelid, G. Tranell, and M. Tangstad: *12th International Ferroalloys Congress, June 6–9, Helsinki, Finland*, 2010, pp. 619–629.
25. H. Dalaker: Doctoral Thesis, NTNU, 2009, p. 215.
26. L. Brewer and D. Mastick: *J. Am. Chem. Soc.*, 1951, vol. 73, p. 2045.
27. F.T. Green and J.L. Margrave: *J. Phys. Chem.*, 1966, vol. 70 (7), pp. 2112–15.
28. J.F. Elliot and M. Gleiser: *Thermochemistry for Steelmaking*, Vol. 1, Addison-Wesley Publishing Company, Inc., Massachusetts, U.S.A., 1960.
29. S.S. Cole and N.W. Taylor: *J. Am. Ceram. Soc.*, 1935, vol. 18, pp. 82–85.
30. R.F. Porter, W.A. Chupka, and M.G. Ingirram: *J. Chem. Phys.*, 1955, vol. 23, pp. 216–17.
31. C.L. Yaws, P.K. Narasimhan, and C. Gabbula: *Yaws' Handbook of Antoine Coefficients for Vapor Pressure*, 2nd ed., Knovel, New York, 2009.
32. A.I. Zaitsev, N.E. Shelkova, N.P. Lyakishev, and B.M. Mogutnov: *Phys. Chem. Chem. Phys.*, 1999, vol. 1, pp. 1899–907.
33. S. Abdelouhab, R. Podor, C. Rapin, M.J. Toplis, P. Berthod, and M. Vilasi: *J. Non-Cryst. Solids*, 2008, vol. 354, pp. 3001–11.
34. K.S. Goto, S. Yamaguchi, and K. Nagata: *Second Int. Symposium on Metallurgical Slags and Fluxes*, H.A. Fine and D.R. Gaskell, eds., Metall. Soc. AIME, New York, 1984, p. 467.
35. J. Safarian and M. Tangstad: *Metall. Mater. Trans. B*, 2012, vol. 43B, pp. 1427–45.
36. T. Shirai, S. Tachibana, and A. Tsuchiyama: *Lunar and Planetary Science XXXI*, Abstract #1610, 2000.